MedChemComm

RESEARCH ARTICLE

View Article Online
View Journal | View Issue

Cite this: *Med. Chem. Commun.*, 2016, 7, 813

Discovery of a novel binding pocket for CYP 2C9 inhibitors: crystallography, pharmacophore modelling and inhibitor SAR†

Sarah E. Skerratt,* Marcel J. de Groot‡ and Chris Phillips§

Received 7th January 2016,
Accepted 3rd February 2016

DOI: 10.1039/c6md00011h

www.rsc.org/medchemcomm

Herein, we describe the discovery of a novel binding pocket for CYP 2C9 inhibitors. Trifluoromethanesulfonamide compounds **1** and **2**, identified within a Pfizer progesterone receptor antagonist program, were found to strongly inhibit the drug metabolizing cytochrome P450 enzyme CYP 2C9. Homology modelling and subsequent X-ray co-crystal data have elucidated the binding orientation of compounds **1** and **2** in CYP 2C9. Compound **2** adopts a previously unreported binding mode. Less acidic sulfonamide analogues within these series have reduced CYP 2C9 activity, and we postulate this is due to a reduced hydrogen bonding potential with key interacting residues within CYP 2C9. This work shows that CYP 2C9 has a more flexible active site than previously reported; therefore multiple binding modes and alternative pharmacophore models must be considered when predicting CYP 2C9 affinity.

Introduction

The progesterone receptor (PR) is a member of the family of ligand-activated transcription factors that includes the estrogen (ER), androgen (AR), glucocorticoid (GR) and mineralocorticoid (MR) receptors. The use of progesterone antagonists for the treatment of a variety of progesterone-related diseases and disorders, such as endometriosis, is of considerable interest to the pharmaceutical industry. In order to identify chemical matter for the Pfizer progesterone receptor antagonist (PRA) program, a high-throughput screening campaign was performed.[1] From this work, a number of chemotypes were selected for lead optimisation, including a cyclohexyl ether and biaryl ether series. Trifluoromethanesulfonamide analogues made within these series were found to be potent antagonists of the progesterone receptor, however they were also found to inhibit the drug metabolizing cytochrome P450 enzyme, CYP 2C9.[2] Examples are shown in Fig. 1. Compound **1**, from the cyclohexyl ether series, is a potent PR antagonist (PR IC_{50} 43 nM), but is also a strong inhibitor of CYP 2C9 (77% I in a CYP 2C9 biochemical assay run at a concentration of 3 μM). Compound **2** from the biaryl ether series is also active at the progesterone receptor (PR IC_{50} of 175 nM) and strongly inhibits CYP 2C9 (95% I in a CYP 2C9 biochemical assay run at a concentration of 3 μM).

CYP 2C9 is a member of the P450 enzyme superfamily of membrane-bound heme-proteins that catalyse the oxidative metabolism of structurally diverse molecules.[2] Of the fifty seven known human P450 isoforms, CYP 2C9 is one of seven isoforms responsible for more than 90% of the metabolism of compounds in current clinical use.[3] However, CYP 2C9 has known human polymorphisms that can lead to rapid or very poor metabolism in specific patient populations.[4–6] In addition, the inhibitory binding of molecules to P450 enzymes such as CYP 2C9 can lead to drug–drug interactions, and may cause severe side effects resulting in the early termination of candidates in development, refusal of approval, prescription limitations or withdrawal of drugs from the market.[7]

Theoretical models that can predict for the possible interaction of drugs or drug candidates with P450 enzymes can be valuable tools in the drug discovery process.[8,9] In order to determine the nature of the protein binding site that interacts with a substrate, a three dimensional representation of the

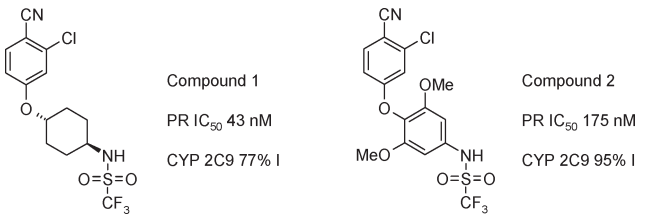

Fig. 1 Structure and properties of compounds **1** and **2**. The CYP 2C9% I data were generated at a 3 μM concentration.

Pfizer Neusentis, The Portway Building, Granta Park, Cambridge, UK.
E-mail: sarah.skerratt@pfizer.com; Tel: +44 (0)1304644073

† The authors declare no competing interests.

‡ Current address: LEO Pharma A/S, 55 Industriparken, 2750 Ballerup, Denmark.

§ Current address: Department of Discovery Sciences, AstraZeneca, Darwin Building, Cambridge Science Park, Milton Road, Cambridge, CB4 0WG, UK.

entire active site is required. For example, rabbit CYP2C5/3, the first mammalian P450 structure to be solved,[10] became the basis of several CYP 2C9 homology models. The publication of crystal structures of the human P450 2C subfamily (Table 1) over recent years has enabled the scientific community to compare previously reported homology models and establish model validity. For example, CYP 2C8 and CYP 2C9 models have been shown to exhibit α-carbon RMS distances of 1.2 Å and 1.5 Å respectively, demonstrating the utility of the CYP 2C5 crystal structure as a template for generating three-dimensional models for other CYP 2C subfamily enzymes.[11–13] Modelling the 3D structure of P450s to allow docking of potential substrates can be a useful method for predicting and rationalising substrate selectivity. It can however be complicated by the fact that multiple ligand binding modes may be available. Several years ago, evidence began to emerge that CYP 3 A4 could bind multiple substrates simultaneously.[14] This observation was later extended to additional P450 enzymes.[15]

With the known risks associated with CYP 2C9 inhibition,[21] the project team sought to design PRA analogues of compounds **1** and **2** with reduced CYP 2C9 liability. To achieve this we desired an understanding of the binding site interactions of compounds **1** and **2** in the CYP 2C9 ligand binding site. In the absence of CYP 2C9 co-crystal structure information, we elected to utilise a CYP 2C9 homology model to guide analogue design.

Results and discussion

CYP 2C9 homology modelling

De Groot *et al.* previously described a CYP 2C9 homology model based on the rabbit CYP2C5/3 crystal structure.[11] This model, and the pharmacophore embedded within, was initially used to predict the potential binding modes of compounds **1** and **2**. In order to dock compounds **1** and **2** into the CYP 2C9 model, the assumption was made that they bind at the same location, and with the same orientation, as substrates in the existing model, such as Flurbiprofen. This orientation consists of a polar/acidic region of the substrate interacting with a positively charged region of the protein (Arg^{108}), a hydrophobic region of the substrate interacting with several hydrophobic protein residues (Phe^{476} and Leu^{362}), and a site of ligand oxidation in close proximity to the heme.

After superposition, the compounds were relaxed using a Macromodel[22] optimization within the confines of the homology model binding pocket. The main binding interactions between compounds **1** and **2** and CYP 2C9 were predicted to be an interaction between the acidic trifluoromethanesulfonamide unit of either compound with CYP 2C9 Arg^{108} and Asn^{204}, as well as hydrophobic interactions between the chlorocyano-phenyl moiety and Phe^{476} and Leu^{362}. The binding orientation also directed the chlorocyano-phenyl groups towards the CYP 2C9 heme moiety (Fig. 2).

Table 1 Available crystal structures of the human P450 2C subfamily

Available crystal structures of the CYP 2C subfamily			
CYP	Resolution (Å)	PDB	Substrate/inhibitor
2C5 (rabbit)	3.00	1dt6 (ref. 10)	None
	2.30	1n6B (ref. 16)	DMZ
	2.10	1nr6 (ref. 17)	Diclofenac
2C8 (human)	2.70	1pq2 (ref. 18)	None
	2.60	2nnh	9-*cis*-Retinoic acid
	2.80	2nni	Montelukast
	2.28	2nnj	Felodipine
	2.70	2vn0	Troglitazone
2C9 (human)	2.60	1og2 (ref. 19)	None
	2.55	1og5 (ref. 19)	*S*-Warfarin
	2.00	1r9O (ref. 20)	Flurbiprofen
	2.45	4nz2	Inhibitor 2QJ
	2.20	4jnm	NAMPT Inhibitors
2C19 (human)	2.87	4gqs	Inhibitor OVX

CYP 2C9 structure–activity-relationships

It is known that CYP 2C9 preferentially binds to hydrophobic molecules that contain an acidic group.[23] A key binding interaction predicted in the homology modelling of compounds **1** and **2** in CYP 2C9 is a hydrogen bond network between the oxygen atoms of the acidic sulfonamide group and polar residues Arg^{108} and Asn^{204} (Fig. 3, compound **1** highlighted only for clarity).

Compound analogues were designed to perturb the strength of the hydrogen bond interaction network with the aim of reducing CYP 2C9 inhibition. Specifically, replacement of the trifluoromethanesulfonamide unit with the less acidic methanesulfonamide group was explored (Fig. 4). Compound **3**, the methanesulfonamide analogue of compound **1**, gratifyingly retained activity at (PR IC_{50} 107 nM) but, unlike compound **1**, was devoid of activity at CYP 2C9 (0% I at 3 μM 2C9). Similarly, compound **4**, the methanesulfonamide analogue of compound **2** maintained activity at the PR receptor (PR IC_{50} 26 nM) and was inactive at CYP 2C9 (9% I at 3 μM 2C9).

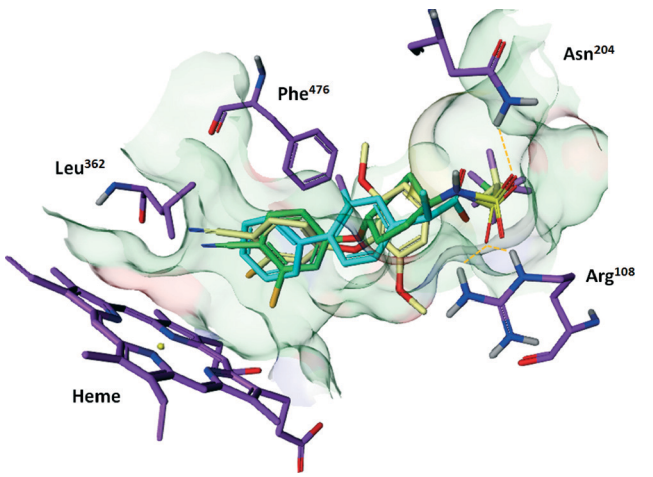

Fig. 2 Superposition of compound **1** (green), compound **2** (yellow) and flurbiprofen (cyan) in the CYP 2C9 homology model binding pocket. Ligand interactions are predicted to be with hydrophobic amino acids Phe^{476} and Leu^{362}, polar residues Arg^{108} and Asn^{204}, and heme group.

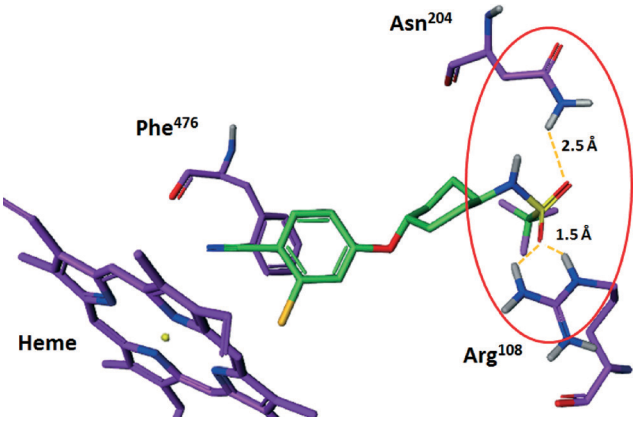

Fig. 3 Predicted hydrogen bonding interactions between sulfonamide oxygens of compound **1** and Arg^{108} and Asn^{204} in the in CYP 2C9 homology model.

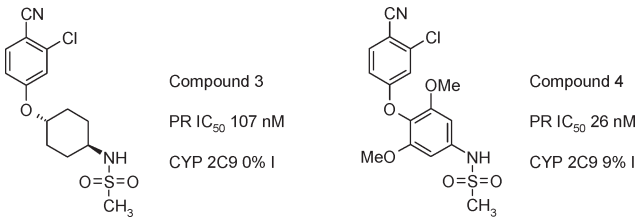

Fig. 4 Structure and properties of compounds **3** and **4**. The CYP 2C9% I data were generated at a 3 μM concentration.

The difference in CYP 2C9 activity between the trifluoromethanesulfonamide compounds and their methanesulfonamide counterparts is intriguing. Each motif is capable of making hydrogen bonding interactions between the sulfonamide oxygen atoms and CYP 2C9 Arg^{108} and Asn^{204} residues, but we postulate that the difference in affinity may be driven by their disparate pK_a values. For example, the measured pK_a of the trifluoromethanesulfonamide unit in compound **1** is 7.0, whereas the pK_a of the methanesulfonamide group in compound **3** is 10.5. As shown in the electrostatic potential plot (Fig. 5) there is a significant increase in negative electrostatic potential on the sulfonamide oxygen atoms when compound **1** exists in the deprotonated (ionized) form relative to the neutral form, the same is true for compound **3** (electrostatic plot not shown). Hence, the increased propensity of compound **1** to exist in the ionic form at neutral (physiologically relevant) pH relative to compound **3**, and drive stronger (charge reinforced) hydrogen bonding with Arg^{108} and Asn^{204}, could explain the enhanced CYP 2C9 activity (the CYP 2C9 assay is run at pH 7.4). The pK_a of compounds **2** and **4** are 4.5 and 8.5 respectively.

CYP 2C9 crystal structures

Co-crystal structures of compounds **1** and **2** with CYP 2C9 were subsequently generated. Compound **1** was shown to bind in a conformation similar to that predicted by the homology model, whereas compound **2** adopted a novel binding conformation. In each case, Arg^{108} interacts with the sulfonamide group, but the orientation of the cyanophenoxy moieties differ. The cyanophenoxy motif of compound **1** faces the heme oxy-iron (binding mode 1), a binding mode consistent with homology modelling data. However, in the co-crystal structure of CYP 2C9 and compound **2**, the cyanophenoxy motif of compound **2** resides in a newly opened hydrophobic pocket, forming a pi-stacking interaction with Phe^{476} (Fig. 6).

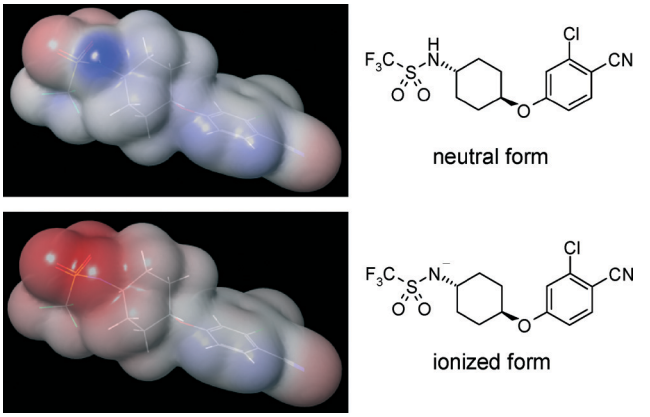

Fig. 5 Electrostatic potential plot of compound **1** in the neutral and ionised state.¶

Comparison of crystal structures with the homology model

The homology model[12] utilised in this work was, in general, in agreement with the CYP 2C9 co-crystal structures generated for compound **2**. One difference noted was the location of the B–C loop region, *i.e.* residues Ile^{88}–Ser^{115},which resided in a more "inward" orientation than in the homology model, and caused by the different conformation of this region in the template used (Fig. 6 shows the location of the BC-loop from crystallographic data). As a consequence, the embedded pharmacophore needed a slight reorientation. This was achieved by a pivot around the site of oxidation along the B–C loop movement vector. Interestingly, despite the movement of the B–C loop, all predicted interactions between the protein and compound **1** were maintained and the results consistent with binding mode 1. As a consequence, the existing homology model could be effectively utilised to predict binding modes of analogues of compound **1**, and guide medicinal chemistry efforts within this series. The binding mode of compound **2** was not correctly predicted by the

¶ Atomic charges are estimated by a least-square fitting of calculated electrostatic potential to potential estimated with electron density derived from quantum mechanical calculation. The surface was created based on an iso-electron density of 0.001. The colour on the surface is associated with sign of the potential, red for negative potential and blue for positive potential. A Jaguar module of Schrodinger suite was used. Calculations were performed on compound conformers identical to the conformation of compound **2** in the CYP 2C9 crystal structure.

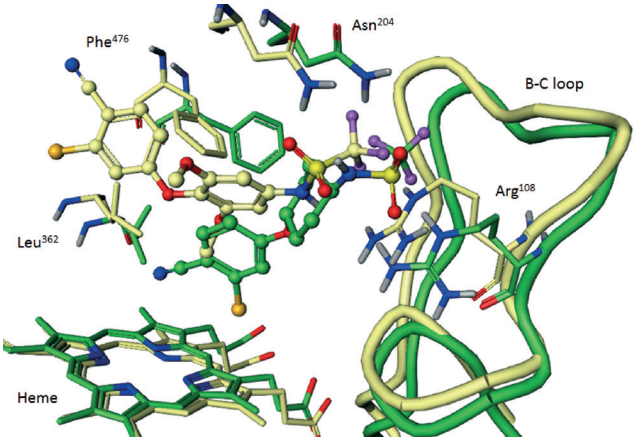

Fig. 6 CYP 2C9 co-crystal structures of compound 1 (green) in binding mode 1 (CYP 2C9 in green) and compound 1 (yellow) in binding mode 2 (CYP 2C9 in yellow).

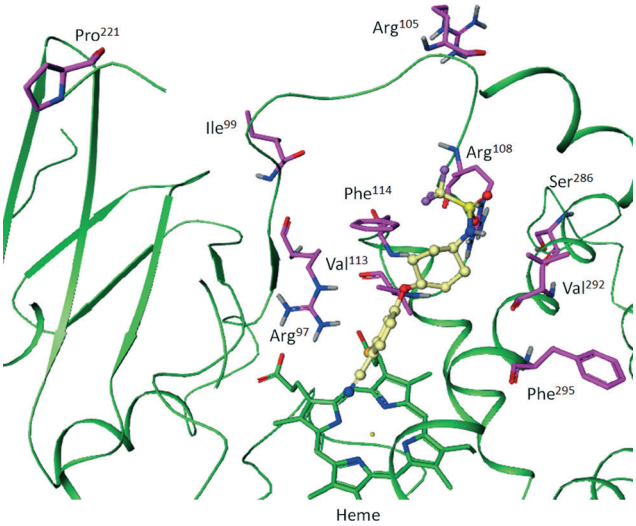

Fig. 7 Compound 1 (yellow) bound to CYP 2C9 (green). The CYP 2C9 residues for which site-directed mutagenesis data are available are highlighted in purple.

existing homology model, and demonstrates CYP 2C9 has a more flexible active site than previously assumed. However, the availability of crystallographic data for this newly observed binding site should enable orthogonal homology models to generated, and enable additional binding modes to be taken into account when predicting potential CYP 2C9 affinity.

Comparison with available site directed mutagenesis data

The influence of various amino acids on the metabolism of CYP 2C9 substrates has previously been examined using site directed mutagenesis (SDM). Mutagenesis in the region of Arg^{105} indicates that this residue is not an important anionic binding site.[24] Mutation of Arg^{97} has an influence on diclofenac metabolism, but Arg^{97} is not predicted to reside in the active site. In our crystal structures, Arg^{97} (Fig. 7) is involved in stabilising the heme propionate moieties.[10,24] Mutation of Arg^{108} to alanine reduces the formation of 4′-hydroxydiclofenac by 100-fold compared with CYP 2C9 wild type. A recent homology model based on the crystal structure of bacterial CYP 102 suggested Arg^{108} is not in the active site,[24] however, in the model for CYP 2C9 used in this work, Arg^{108} is an essential part of the CYP 2C9 active site.[12] Our current crystal structures confirm that Arg^{108} plays a key role in the interaction with the acidic part of the inhibitors used in this study.

Recent SDM experiments designed to confer (*S*)-mephenytoin activity at CYP 2C9 suggested activity is dictated by amino acids that influence the packing of structural elements or influence substrate access to the channel, rather than altering the active site directly (Ile^{99} in the B′-region, Ser^{220} and Pro^{221} in the F–G-loop and Ser^{286}, Val^{292} and Phe^{295} in the I-helix, none of which are in direct contact with (*S*)-mephenytoin).[25] Our crystal structures agree that none of these residues seem to be directly interacting with our co-crystallised inhibitors, or the modelled locations of the substrates.

Mutagenesis experiments guided by homology modelling and CoMFA analysis suggest B′–C helix loop residues Phe^{114} and Val^{113} can make hydrophobic interactions with substrates.[26] Our crystal structures support these data.

Compound synthesis

The synthetic routes towards compounds 1 and 3 are described in Scheme 1. Deprotonation of cyclohexanol 6 with NaH in THF followed by addition of fluorobenzonitrile 6 furnished cyclohexylamine 7 in good yield. Compound 1 was synthesised by triflation of cyclohexylamine 7 using triflic anhydride and triethylamine in DCM at −60 °C (79% yield). Compound 3 was made by addition of methanesulfonyl

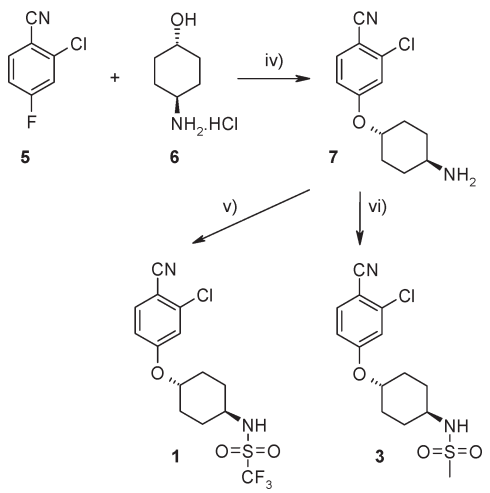

Scheme 1 Synthesis of ethers 1 and 3. Reagents and conditions: iv) NaH, THF, 25 °C, 79%. v) Tf_2O, Et_3N, DCM, −60 °C, 5 min, 92%; v) MsCl, Et_3N, DCM, 25 °C, 1 h, 95%.

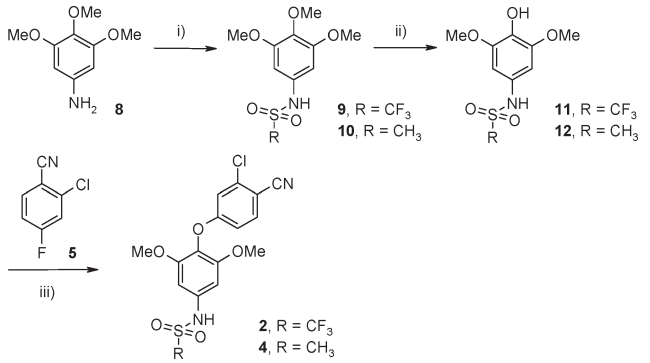

Scheme 2 Synthesis of aryl ethers **2** and **4**. Reagents and conditions: where R = SO_2CF_3 i) Tf_2O, Et_3N, DCM, −78 °C, 3 h, 76%. Where R = SO_2CH_3, i) MsCl, Et_3N, DCM, 25 °C, 2 h, 85%; ii) TMSI, DCM, 25 °C, 3 h, 88–89%; iii) Cs_2CO_3, NMP, 120 °C, 10 h, 85–89%.

chloride and triethylamine to **7** in dichloromethane and pyridine (95% yield).

Compounds **2** and **4** were prepared by a three-step sequence as described in Scheme 2. Aniline **8** was derivatized under standard conditions using trifluoromethanesulfonic anhydride to furnish sulfonamide **9** in 76% yield. Regioselective demethylation of **9** with trimethylsilyl iodide afforded phenol **11** in 88% yield.[23] Subsequent etherification of **11** *via* addition of aryl fluoride **5** under basic conditions furnished compound **2** in an 85% yield. Compound **4** was prepared in a similar manner. Mesylation of **8** with methanesulfonyl chloride in triethylamine and DCM afforded sulfonamide **10** in 85% yield. Demethylation of **10** with trimethylsilyl iodide gave phenol **12** (89% yield) and subsequent etherification *via* addition of aryl fluoride **5** furnished compound **4** (89% yield).

Conclusions

Trifluoromethanesulfonamide compounds **1** and **2**, identified within a progesterone receptor antagonist program, were found to strongly inhibit the drug metabolizing cytochrome P450 enzyme CYP 2C9. In order to design analogues with reduced CYP 2C9 activity, a CYP 2C9 homology model previously described by De Groot *et al.* was used to predict the potential binding modes of compounds **1** and **2**. The modelling predicted a key binding determinant to be a hydrogen bond network made between the two sulfonamide oxygen atoms of the ligands and Arg^{108} and Asn^{204} of CYP 2C9.

Electrostatic mapping showed a significant increase in negative electrostatic potential on the sulfonamide oxygen atoms in the ionized *versus* the neutral form, and we reasoned the interaction of CYP 2C9 with the ionized form of the sulfonamide group would lead to increased CYP 2CP binding through an enhanced hydrogen bonding interaction. We therefore synthesised less acidic sulfonamide analogues such that, at physiological pH, the propensity of the sulfonamide motif to exist in an ionized form would be reduced. Methanesulfonamide compounds **3** and **4** were synthesised and, gratifyingly, they retained activity at the progesterone receptor but lost their inhibitory effects at CYP 2C9.

Subsequent X-ray crystal structure work fully elucidated the binding orientation of progesterone receptor antagonist compounds **1** and **2** in CYP 2C9. Significantly, the co-crystal structure with compound **2** in CYP 2C9 identified a novel and unpredicted binding mode in which a conformational change is induced, re-ordering Phe^{476}, and opening up a hydrophobic pocket. This work shows that CYP 2C9 has a more flexible active site than previously assumed. The crystallographic data for the newly observed binding site should enable orthogonal homology models to be generated, and enable additional binding modes to be taken into account when predicting CYP 2C9 affinity.

Experimental section

All commercially available chemicals and solvents were used without further purification. All temperatures are in °C. Flash column chromatography was carried out using Merck silica gel 60 (9385) or Redisep silica. NMR spectra were obtained on a Varian Mercury (400 MHz) or a Bruker Avance (400 MHz) using the residual signal of the deuterated NMR solvent as the internal reference. Chemical shifts are expressed in parts per million (ppm), multiplicity of the signals are indicated by lower-case letters (singlet s, doublet d, triplet t, quadruplet q, multiple m, broad singlet br s), and deuterated solvents are dimethylsulfoxide d_6, methanol d_4, and chloroform d_1. Mass spectral date were obtained using Waters ZQ ESCI or Applied Biosystem's API-2000.

4-[(*trans*-4-Aminocyclohexyl)oxy]-2-chlorobenzonitrile (7)

To a stirred suspension of **6** (486 mg, 3.22 mmol) in dry THF (200 mL) was added NaH (170 mg, 7.11 mmol) portion-wise. The resulting mixture was stirred at 25 °C for 10 min after which time **5** (500 mg, 3.22 mmol) was added. The reaction mixture was heated to 70 °C and stirred for 2 h. After cooling to room temperature, the mixture was poured onto ice (100 g) and extracted with EtOAc (3 × 50 mL). The combined organics were washed with 3 N $HCl_{(aq.)}$ (5 × 50 mL), the combined acidic extracts basified to pH 8 with 3 N $NaOH_{(aq.)}$ and extracted with EtOAc (3 × 30 mL). The combined organics were washed with water (30 mL), dried over $MgSO_4$ and concentrated *in vacuo* to afford the title compound as off-white solid (635 mg, 79% yield). *m*/*z* 251 [M + H, $^{35}Cl]^+$, 253 [M + H, $^{37}Cl]^+$.

N-[*trans*-4-(3-Chloro-4-cyanophenoxy)cyclohexyl]-1,1,1-trifluoromethanesulfonamide (1)

To a stirred solution of **7** (250 mg, 1.00 mmol) and triethylamine (207 μL, 1.50 mmol) in DCM (25 mL) at −60 °C was added triflic anhydride (168 μL, 1.00 mmol). The reaction mixture was stirred for 1 h, then poured onto water (25 mL) and extracted with DCM (2 × 25 mL). The combined organics were washed with water (25 mL), dried over $MgSO_4$ and

concentrated *in vacuo*. The residue was purified *via* silica gel column chromatography (eluting with 25% EtOAc/75% hexane) to afford the title compound as a white crystalline solid (211 mg, 79% yield). *m*/*z* 383 $[M + H]^+$.

N-[*trans*-4-(3-Chloro-4-cyanophenoxy)cyclohexyl]-methanesulfonamide (3)

To a stirred solution of 7 (130 mg, 0.52 mmol) in DCM (5 mL) and pyridine (1 mL) at 25 °C, was added methaneulfonyl chloride (77 μL, 1 mmol). The resulting mixture was stirred at 25 °C for 2 h, poured onto 2 N $HCl_{(aq.)}$ (10 mL) and extracted with DCM (2 × 10 mL). The combined organics were washed with water (10 mL), brine (10 mL), dried over $MgSO_4$ and concentrated *in vacuo*. The residue was purified *via* silica gel column chromatography (eluting with 45% EtOAc/55% hexane) to afford the title compound as a white solid (162 mg, 95% yield). *m*/*z* 346 $[M + NH_4]^+$.

1,1,1-Trifluoro-*N*-(3,4,5-trimethoxyphenyl)methanesulfonamide (9)

To a stirred solution of 8 (1.00 g, 5.46 mmol) and triethylamine (0.93 mL, 6.60 mmol) in DCM (20 mL) at −78 °C was added triflic anhydride (0.11 mL, 6.60 mmol). The reaction mixture was stirred for 1 h and then poured onto water (25 mL) and extracted with DCM (2 × 20 mL). The combined organics were washed with brine (25 mL), dried over $MgSO_4$ and concentrated *in vacuo*. The residue was purified *via* silica gel column chromatography (eluting with 50% EtOAc/50% hexane) to afford the title compound as a white crystalline solid (1.64 g, 79% yield). ^{1}H NMR (400 MHz, $CDCl_3$) δ: 3.85 (s, 9H), 6.50 (s, 2H), 6.80 (br s, 1H).

N-(3,4,5-Trimethoxyphenyl)methanesulfonamide (10)

To a stirred solution of 8 (5.00 g, 27.3 mmol) in DCM (10 mL) and pyridine (2 mL) at 25 °C, was added methaneulfonyl chloride (2.1 mL, 27.3 mmol). The resulting mixture was stirred at 25 °C for 2 h, poured onto 2 N $HCl_{(aq.)}$ (100 mL) and extracted with DCM (2 × 75 mL). The combined organics were washed with water (100 mL), brine (100 mL), dried over $MgSO_4$ and concentrated *in vacuo*. The residue was purified *via* silica gel column chromatography (eluting with 30% EtOAc/70% hexane) to afford the title compound as an off-white solid (6.06 g, 85% yield). ^{1}H NMR (400 MHz, $CDCl_3$) δ: 3.00 (s, 3H), 3.90 (s, 9H), 6.40 (br s, 1H), 6.50 (s, 2H).

1,1,1-Trifluoro-*N*-(4-hydroxy-3,5-dimethoxyphenyl)methanesulfonamide (11)

To a stirred solution of 9 (1.30 g, 4.13 mmol) in DCM (10 mL) at 0 °C was added TMSI (1.76 mL, 12.4 mmol) and the resulting mixture warmed to 20 °C and stirred for 3 h. 20 mL of a 1 : 1 water/acetone mix was then added and the resulting mixture extracted with EtOAc (2 × 30 mL). The combined organics were washed with brine (30 mL), dried over $MgSO_4$ and concentrated *in vacuo* to give the title compound as a white solid (3.28 g, 88%). ^{1}H NMR (400 MHz, $CDCl_3$) δ: 3.90 (s, 6H), 5.60 (br s, 1H), 6.55 (s, 2H), 6.75 (br s, 1H).

N-(4-Hydroxy-3,5-dimethoxyphenyl)methanesulfonamide (12)

To a stirred solution of 10 (1.59 g, 6.1 mmol) in DCM (10 mL) at 0 °C was added TMSI (2.65 mL, 18.3 mmol) and the resulting mixture warmed to 20 °C and stirred for 3 h. 20 mL of a 1 : 1 water/acetone mix was then added and the resulting mixture extracted with EtOAc (2 × 50 mL). The combined organics were washed with brine (50 mL), dried over $MgSO_4$ and concentrated *in vacuo* to afford the title compound as a white solid (1.34 g, 89%). ^{1}H NMR (400 MHz, $CDCl_3$) δ: 3.00 (s, 3H), 3.90 (s, 6H), 5.45 (br s, 1H), 6.30 (br s, 1H), 6.55 (s, 2H).

N-[4-(3-Chloro-4-cyanophenoxy)-3,5-dimethoxyphenyl]-1,1,1-trifluoromethanesulfonamide (2)

To a stirred solution of 11 (250 mg, 0.83 mmol) in NMP (5 mL) was added 5 (142 mg, 0.91 mmol) followed by Cs_2CO_3 (809 mg, 2.49 mmol) and the resulting mixture heated to 120 °C for 12 h. After this time the mixture was portioned between water (10 mL) and EtOAc (10 mL). The aqueous layer was further extracted with EtOAc (2 × 20 mL) and the combined organics washed with brine (10 mL), dried over $MgSO_4$, and concentrated *in vacuo*. The residue was purified *via* silica gel column chromatography, eluting with 50% EtOAc/50% pentane) to afford the title compound as a white solid (307 mg, 85% yield). ^{1}H NMR (400 MHz, DMSO-d_6) δ: 3.72 (s, 6H), 6.64 (s, 2H), 6.83–6.85 (m, 1H), 7.13–7.14 (m, 1H), 7.83–7.85 (m, 1H); *m*/*z* 239 $[M + H]^+$; *m*/*z* 435 $[M - H]^-$.

N-[4-(3-Chloro-4-cyanophenoxy)-3,5-dimethoxyphenyl]-methane sulfonamide (4)

To a stirred solution of 12 (250 mg, 1.01 mmol) in NMP (3 mL) was added 5 (186 mg, 1.2 mmol) followed by Cs_2CO_3 (715 mg, 2.2 mmol) and the resulting mixture heated to 120 °C for 10 h. After this time the mixture was portioned between water (10 mL) and EtOAc (10 mL). The aqueous layer was further extracted with EtOAc (2 × 10 mL) and the combined organics washed with brine (20 mL), dried over $MgSO_4$, and concentrated *in vacuo*. The residue was purified *via* silica gel column chromatography, eluting with 50% EtOAc/50% pentane) to afford the title compound as a white solid (343 mg, 89% yield). ^{1}H NMR (400 MHz, $CDCl_3$) δ: 3.10 (s, 3H), 3.80 (s, 6H), 6.40 (br s, 1H), 6.55 (s, 2H), 6.85 (dd, 1H), 6.95 (d, 1H), 7.55 (d, 1H); *m*/*z* 381 $[M - H]^-$.

Crystallography

Following the methods of Wester *et al.* (2004) an engineered construct containing residues 23–489 of the catalytic domain of human 2C9 with the first 22 residues replaced with the sequence MAKKT was over-expressed in *E. coli* and purified using the two column method previously described.[17] Crystals were grown using the hanging drop vapour diffusion

method in conditions essentially equivalent to those reported. The crystals are isomorphous with pdb deposition 1R9O, belonging to space group *R*3 with a unit cell of $a = b = 91.1$ Å, $c = 169.5$ Å and can be produced using a co-crystallization method, with ligands at a concentration of 5 mM incubated with the protein on ice for 30 minutes prior to crystallization set-up. Data were collected at beamline ID23 of the ESRF to a resolution of 2 Å for the complex with compound **1** and on an 'in house' Rigaku FRD X-ray source with a Saturn92 CCD camera for the complex with compound **2**. Data were reduced and scaled using the XDS and the CCP4 suite of programs,[24] iterative rounds of model building preformed in COOT,[25] and refined with BUSTER.[26] The coordinates and reflection data have been deposited with the PDB with the accession codes: 5a5i and 5a5j respectively.

Acknowledgements

The authors would like to thank Mr. Toby Underwood and Dr. Paul A. Bradley for synthesis of the compounds described in this publication, Dr. Kiyoyuki Omoto for generating the electrostatic potential maps of compounds **2** and **3**, Dr. Steve Irving for protein purification and Mr. Alec Tucker for protein crystallization.

Notes and references

1 K. N. Dack, *et al.*, Optimisation of a pyrazole series of progesterone antagonists; Part 1, *Bioorg. Med. Chem. Lett.*, 2010, **20**(11), 3384–3386.
2 D. R. Nelson, *et al.*, P450 superfamily: update on new sequences, gene mapping, accession numbers and nomenclature, *Pharmacogenetics*, 1996, **6**, 1–42.
3 D. A. Smith and B. C. Jones, Speculations on the substrate structure–activity relationship (SSAR) of cytochrome P450 enzymes, *Biochem. Pharmacol.*, 1992, **44**(11), 2089–2098.
4 T. H. Sullivan-Klose, *et al.*, The role of the CYP 2C9-Leu359 allelic variant in the tolbutamide polymorphism, *Pharmacogenetics*, 1996, **6**(4), 341–349.
5 G. P. Aithal, *et al.*, Association of polymorphisms in the cytochrome P450 CYP 2C9 with warfarin dose requirement and risk of bleeding complications, *Lancet*, 1999, **353**(9154), 717–719.
6 R. S. Kidd, *et al.*, Identification of a null allele of CYP 2C9 in an African-American exhibiting toxicity to phenytoin, *Pharmacogenetics*, 2001, **11**(9), 803–808.
7 C. C. Ogu and J. L. Maxa, Drug interactions due to cytochrome P450, *Proc. (Bayl. Univ. Med. Cent.)*, 2000, **13**(4), 421–423.
8 M. J. de Groot, S. B. Kirton and M. J. Sutcliffe, In silico methods for predicting ligand binding determinants of cytochromes P450, *Curr. Top. Med. Chem.*, 2004, **4**(16), 1803–1824.
9 M. J. de Groot, S. B. Kirton and M. J. Sutcliffe, In Silico methods for predicting ligand binding determinants of cytochromes P450 (Cytochromes P450s in Medicinal Chemistry and Drug Discovery), in *Frontiers in Medicinal Chemistry*, DOI: 10.2174/978160805206610603010615.
10 P. A. Williams, *et al.*, Mammalian microsomal cytochrome P450 monooxygenase: structural adaptations for membrane binding and functional diversity, *Mol. Cell*, 2000, **5**, 121–131.
11 M. J. de Groot, A. A. Alex and B. C. Jones, Development of a combined protein and pharmacophore model for CYP 2C9, *J. Med. Chem.*, 2002, **45**(10), 1983–1993.
12 L. Afzelius, *et al.*, Structural analysis of CYP 2C9 and CYP2C5 and an evaluation of commonly used molecular modeling techniques, *Drug Metab. Dispos.*, 2004, **32**, 1218–1229.
13 L. Afzelius, *et al.*, Conformer- and alignment-independent model for predicting structurally diverse competitive CYP 2C9 inhibitors, *J. Med. Chem.*, 2004, **47**(4), 907–914.
14 M. Shou, *et al.*, Activation of CYP3A4: evidence for the simultaneous binding of two substrates in a cytochrome P450 active site, *Biochemistry*, 1994, **33**(21), 6450–6455.
15 K. R. Korzekwa, *et al.*, Evaluation of atypical cytochrome P450 kinetics with two-substrate models: evidence that multiple substrates can simultaneously bind to cytochrome P450 active sites, *Biochemistry*, 1998, **37**(12), 4137–4147.
16 M. R. Wester, *et al.*, Structure of a substrate complex of mammalian cytochrome P450 2C5 at 2.3 Å resolution: evidence for multiple substrate binding modes, *Biochemistry*, 2003, **42**(21), 6370–6379.
17 M. R. Wester, *et al.*, Structure of mammalian cytochrome P450 2C5 complexed with diclofenac at 2.1 Å resolution: evidence for an induced fit model of substrate binding, *Biochemistry*, 2003, **42**(31), 9335–9345.
18 G. A. Schoch, *et al.*, Structure of human microsomal cytochrome P450 2C8. Evidence for a peripheral fatty acid binding site, *J. Biol. Chem.*, 2004, **279**(10), 9497–9503.
19 P. A. Williams, *et al.*, Crystal structure of human cytochrome P450 2C9 with bound warfarin, *Nature*, 2003, **424**, 464–468.
20 M. R. Wester, *et al.*, The structure of human cytochrome P450 2C9 complexed with flurbiprofen at 2.0-Å resolution, *J. Biol. Chem.*, 2004, **279**(34), 35630–35637.
21 J. O. Miners and D. J. Birkett, Cytochrome P4502C9: an enzyme of major importance in human drug metabolism, *Br. J. Clin. Pharmacol.*, 1998, **45**(6), 525–538.
22 E. Schrödinger, *Macromodel*, Schrödinger, New York, 2006.
23 D. R. McMasters, *et al.*, Inhibition of Recombinant Cytochrome P450 Isoforms 2D6 and 2C9 by Diverse Drug-like Molecules, *J. Med. Chem.*, 2007, **50**(14), 3205–3213.
24 M. Ridderström, *et al.*, Arginines 97 and 108 in CYP 2C9 are important determinants of the catalytic function, *Biochem. Biophys. Res. Commun.*, 2000, **270**(3), 983–987.
25 C.-C. Tsao, *et al.*, Identification of human CYP2C19 residues that confer S-mephenytoin 4′-hydroxylation activity to CYP 2C9, *Biochemistry*, 2001, **40**(7), 1937–1944.
26 R. L. Haining, *et al.*, Enzymatic determinants of the substrate specificity of CYP 2C9: Role of B'-C loop residues in providing the p-stacking anchor for warfarin binding, *Biochemistry*, 1999, **38**(11), 3285–3292.